

1 **Submit to: ISME Journal**

2

3 **Declines in ice cover induce light limitation in freshwater diatoms**

4

5

6 Brittany N. Zepernick¹, Emily E. Chase¹, Elizabeth R. Denison¹, Naomi E. Gilbert^{1#}, Robbie M.
7 Martin¹, Alexander R. Truchon¹, Thijs Frenken^{2,6}, William R. Cody³, Justin D. Chaffin⁴, George
8 S. Bullerjahn⁵, R. Michael L. McKay^{6*} and Steven W. Wilhelm^{1*}

9

10 ¹Department of Microbiology, The University of Tennessee, Knoxville, Tennessee, USA

11 ²HAS University of Applied Sciences, 's-Hertogenbosch, The Netherlands

12 ³Aquatic Taxonomy Specialists, Malinta, OH, United States

13 ⁴Stone Laboratory and Ohio Sea Grant, The Ohio State University, Put-In-Bay, Ohio USA

14 ⁵Department of Biological Sciences, Bowling Green State University, Bowling Green, Ohio, USA

15 ⁶Great Lakes Institute for Environmental Research, University of Windsor, Windsor, Ontario, Canada

16

17 [#]Current Affiliation: Lawrence Livermore National Laboratory, Livermore, CA, USA

18

19

20

21

22

23

24

25

26

27

28

29

30

31

32 ***Correspondence:**

33

34 Steven W. Wilhelm, wilhelm@utk.edu, 1-865-974-0665

35 Robert. M. McKay, robert.mckay@windsor.ca, 1-519-253-3000 x 2797

36

37 **Running title:** Evidence of the light limitation hypothesis in the ice-free water column

38 **Key Words:** Winter Limnology, Metatranscriptomics, Great Lakes, Climate Change,
39 Bacillariophyta

40

41 **Abstract (250 words)**

42 The rediscovery of diatom blooms embedded within and beneath Lake Erie ice cover
43 (2007-2012) ignited an intense interest in psychrophilic adaptations and winter limnology.
44 Subsequent studies determined ice plays a vital role in winter diatom ecophysiology, as diatoms
45 partition to the underside of ice thereby fixing their location within the photic zone. Yet, climate
46 change has led to widespread ice decline across the Great Lakes, with Lake Erie presenting a
47 nearly ice-free state in several recent winters. It has been hypothesized the resultant turbid,
48 isothermal water column will induce light limitation amongst winter diatoms, serving as a
49 detrimental competitive disadvantage. Here, we conducted a physiochemical and
50 metatranscriptomic survey of the winter Lake Erie water column (2019-2020) that spanned
51 spatial, temporal, and climatic gradients to investigate this hypothesis. We determined ice-free
52 conditions decreased diatom bloom magnitude and altered diatom community composition.
53 Diatoms increased the expression of various photosynthetic genes and iron transporters,
54 suggesting they are attempting to increase their quantity of photosystems and light-harvesting
55 components (a well-defined indicator of light limitation). Notably, we identified two gene
56 families which serve to increase diatom fitness in the turbid ice-free water column: proton-
57 pumping rhodopsins (a second means of light-driven energy acquisition) and fasciclins (a means
58 to “raft” together to increase buoyancy and co-locate to the surface to optimize light acquisition).
59 With large-scale climatic changes already underway, our observations provide insight into how
60 diatoms respond to the dynamic ice conditions of today and shed light on how they will fare in a
61 climatically altered tomorrow.

62

63

64 **Introduction**

65 Winter was historically considered a period of planktonic persistence rather than growth
66 [1, 2]. Yet, a series of limnological surveys conducted in the winters of 2007-2012 contested this
67 with the rediscovery of dense diatom blooms associated with ice cover of Lake Erie (US,
68 Canada) [3, 4]. This finding ignited interest in winter limnology [5-7], with subsequent studies
69 demonstrating ice-associated communities were dominated by the centric colonial diatoms
70 *Aulacoseira islandica* and *Stephanodiscus* spp. [3, 4, 8-10]. Notably, chlorophyll *a* (Chl *a*)
71 concentrations during winter surpassed those of spring [3] and examinations of silica deposition
72 in frustules demonstrated cells were metabolically active [11]. Additional studies emphasized
73 these blooms are of biotic and biogeochemical importance, as winter-spring diatom biovolumes
74 surpass summer cyanobacterial biovolumes by 1.5- to 6-fold [12] and drive recurrent summer
75 hypoxia in the Lake Erie central basin [7, 10, 12]. Though Lake Erie serves as a leading case
76 study for winter diatom blooms, they are far from an isolated phenomenon. Blooms are often
77 unreported due to a lack of winter surveys [13], yet they have been well-documented beneath the
78 ice in Lake Baikal [14, 15] and characterized in other north temperate freshwater systems such as
79 The Loch (US) [16], Lake Barleber (Germany) [13], Lakes Ladoga and Onega (Russia) [17],
80 Lake Kasumigaura (Japan) [18] and the River Danube (Hungary) [19].

81 Contributing to the ecological success of winter diatoms are adaptations that increase
82 membrane fluidity and enhance light harvesting in icy, low-light conditions [9]. Yet, arguably a
83 major adaptation responsible for winter diatom success is their ability to partition to surface ice
84 cover *via* interactions with ice-nucleating bacteria, which allows diatoms to co-locate themselves
85 to the under-ice surface to maintain an optimal light climate for photosynthesis [8, 20].
86 Cumulatively, studies demonstrate ice cover plays a critical role in shaping winter diatom

87 ecophysiology and increasing competitive fitness in the icy water column [3, 4, 8, 9, 11, 20].
88 Yet, this raises the question of how this keystone phyla [21-24] will fair in a climatically altered
89 ice-free future.

90 Lake Erie, concomitantly with other lakes across the globe, is experiencing
91 unprecedented declines in ice cover [7, 25, 26]. Notably, projections suggest ice cover may
92 disappear entirely across the Great Lakes by the end of the century [27]. This loss of ice cover
93 presents a unique scenario for shallow lakes such as Erie (mean depth ~19 m). Due to
94 predominant westerly winds blowing across the lakes west-to-east axis, snow seldomly
95 accumulates on the surface ice [3, 20, 28] (Figure 1A), allowing light to penetrate below ice
96 cover where diatoms are located. Yet, in the absence of ice cover, winds create an isothermal
97 turbid water column in this shallow lake [29, 30] (Figure 1B). Indeed, Beall et al., [4] reported
98 turbidities (NTU) a magnitude higher in ice-free Lake Erie (2012) compared to the ice-covered
99 year prior (2011), and noted diatom abundances significantly declined in the turbid water
100 column. This study suggested light limitation was the key driver of diatom decline, citing
101 elevated turbidity within an ice-free lake would induce light limitation [4, 7, 31, 32].

102 We employed *in situ* analyses and metatranscriptomics to explore the hypothesis that
103 winter diatoms are light limited in the ice-free water column. Facilitated by collaborative efforts
104 with the U.S. and Canadian Coast Guards [33], opportunistic samples were collected throughout
105 2019 and 2020, yielding winter samples collected from both ice-covered (2019) and ice-free
106 (2020) water columns [34]. The survey also included spring samples (outgroup). Our analyses
107 confirm ice cover alters diatom bloom magnitude and phylogeny while providing novel evidence
108 of light limitation within diatom communities of the ice-free water column. We also present

109 evidence of two adaptations which we hypothesize increase the competitive fitness of freshwater
110 diatoms within the ice-free winter water column.

111

112 **Methods**

113 *Lake Erie winter-spring water column sampling*

114 Samples of opportunity (n = 77) from the Lake Erie planktonic community were
115 collected across temporal, spatial, and climatic gradients throughout the winter of 2019 and
116 2020. This large-scale collaborative effort included multiple surveys conducted by USCGC *Neah*
117 *Bay*, CCGS *Limnos* and M/V *Orange Apex*, resulting in a large metatranscriptomic dataset [34].
118 Prior to sample collection, water column physiochemical parameters were recorded along with
119 meteorological conditions and ice cover observations. Briefly, water samples were collected
120 from 0.5 m below the surface and processed for analyses of dissolved and particulate nutrients
121 (mg L⁻¹), size-fractionated (< 0.22-μm and < 20 μm) Chl *a* biomass (μg L⁻¹), phytoplankton
122 taxonomy and enumeration (cells L⁻¹), and total community RNA. Metadata are available online
123 at the Biological and Chemical Oceanography Data Management Office (BCO-DMO) [35].
124 Refer to Supplemental Methods/Results and Supplemental Tables for further details.

125

126 *RNA extraction and sequencing*

127 RNA extractions were performed using previously described phenol-chloroform methods
128 with ethanol precipitation [36]. Residual DNA in samples was digested *via* a modified version of
129 the Turbo DNase protocol using the Turbo DNA-free kit (Ambion, Austin, TX, USA). Samples
130 were determined to be DNA-free *via* the absence of a band in the agarose gel after PCR
131 amplification using 16S rRNA primers as previously reported [34]. Samples were quantified

132 using the Qubit RNA HS Assay Kit (Invitrogen, Waltham, MA, USA) and sent to the
133 Department of Energy Joint Genome Institute (DOE JGI) for ribosomal RNA reduction and
134 sequencing using an Illumina NovaSeq S4 2 × 151-nucleotide indexed run protocol (15 million
135 150-bp paired-end reads per library) as reported previously [34].

136

137 *Metatranscriptomic analysis*

138 Filtering and trimming of raw reads was performed by DOE JGI using BBduk (v.38.92)
139 and BBMap (v.38.86) [37, 38]. Bioinformatic processing was conducted using a prior-
140 established metatranscriptomic workflow [39]. Trimmed and filtered libraries (n = 77) were
141 concatenated and assembled (co-assembled) using MEGAHIT (v.1.2.9) [40]. Co-assembly
142 statistics were determined *via* QUAST QC (v.5.0.2) [41]. Trimmed reads were mapped to the co-
143 assembly using BBMap (default settings) (v.38.90) [38]. Gene predictions within the co-
144 assembly were called using MetaGeneMark (v.3.38) [42] using the metagenome style model.
145 Taxonomic annotations of predicted genes were determined using the MetaGeneMark protein
146 file, EUKulele (v.1.0.6) [43] and the PhyloDB (v.1.076) database. We note, this study brings to
147 light a challenge within the freshwater field at large: there is a lack of sequenced freshwater
148 diatom taxa and an absence of freshwater taxonomic annotation databases, which constrains the
149 taxonomic resolution of bioinformatic data. Indeed, in 2016, Edgar et al., [9] noted only 23% of
150 the taxonomic diatom annotations within their Lake Erie metatranscriptome could be tied to
151 genera known to be present within the Great Lakes. Earlier this year, Reavie [44] reiterated the
152 lack of studies regarding Great Lakes diatoms, citing there are various undescribed and
153 unclassified diatom taxa to date. As a result, there may be transcriptional changes within the
154 winter diatom community which have gone undetected within this study, specifically at the

155 genera level. Many of the taxonomic annotations we generated were best aligned to marine
156 counterparts due to a lack of sequenced freshwater representatives (*i.e.*, where reads are
157 annotated as belonging to a genus “-like” genome). More broadly, sequence data is often not
158 coincident with classic morphological taxonomy. Nonetheless, *A. islandica* filaments exhibit a
159 distinct morphology from *Stephanodiscus* spp., and bioinformatic pipelines such as EUKulele
160 accurately distinguish the taxonomy of these “unsung eukaryotes” at the class level [43]. Thus,
161 this ambiguity in diatom taxonomy does not negate the definitive disparity in diatom cell counts
162 and transcription observed in this study. Following, genes were functionally annotated using
163 eggNOG-mapper using a specified e-value of 1e⁻¹⁰ (v.2.1.7) [45]. Ensuing, featureCounts [46]
164 within the subread (v.2.0.1) package was used to tabulate read counts to predicted genes.
165 Mapped reads were normalized to TPM (Transcripts Per Million), representing relative
166 “expression” values prior to statistical analyses (ANOSIM, SIMPER, nMDS etc.). To investigate
167 transcriptional patterns of the winter diatom bloom community, we focused on a subset of
168 libraries (n = 20) selected for consistency in sample collection methods (whole water filtration)
169 and diatom abundances (Supplemental Table 1). Thus, all data reported hereafter pertains to
170 these 20 libraries. Raw data for all 77 transcriptomic libraries are available at the JGI Data Portal
171 (<https://data.jgi.doe.gov>) under Proposal ID 503851 [34]. Refer to Supplemental
172 Methods/Results and Supplemental Tables for further details.

173

174 *Phylogenetic analysis*

175 A phylogenetic tree of fasciclin containing domains (proteins of interest) was produced
176 using differentially expressed (DE) putative proteins identified from this study (n=18), domains
177 recovered from the eggNOG orthology database and publicly available domains from NCBI

178 [47]. A custom database was curated using all NCBI diatom proteins. A DIAMOND (v.2.0.15)
179 [48] blastp alignment was performed with putative fasciclin proteins and eggNOG domains
180 against the diatom database to recover all putative diatom fasciclin domains. The recovered
181 domains were then aligned (DIAMOND blastp) against the NCBI non-redundant database. These
182 results were compiled and collapsed to 80% similarity using CD-HIT (v.4.7) [49] and a multiple
183 sequence alignment was performed using MAFFT (v.7.310) [50] with 500 iterations. Gaps were
184 closed using trimAl with gappyout (v.1.4.rev15) [51] and examined using AliView (v.1.28) [52].
185 A phylogenetic tree (1000 bootstraps) was constructed using a model test selecting for a general
186 non-reversible Q matrix model estimated from Pfam database (v. 31) [53] with a gamma rate
187 heterogeneity. The consensus tree was visualized using iTOL [54].

188 A phylogenetic tree of diatom PPR containing domains (proteins of interest) was
189 produced using DE (n = 2) and non-DE (n = 9) putative proteins identified from this study (total
190 n=11), NCBI non-redundant database (nr) putative proteins were searched using baited study
191 sequences identified as rhodopsin/rhodopsin-like/rhodopsin and with a diatom taxonomic
192 designation by EUKulele via diamond blastp (v. 2.0.15), the NCBI nr database was queried
193 again with these results. NCBI nr was also queried in the same way with potential freshwater
194 diatom whole genomes with no suitable results. Retrieved amino acid sequences were collapsed
195 at 100% using CD-HIT and aligned by MAFFT (v.7.520) with 1000 iterations. The alignment
196 was then trimmed using trimAL (v.1.4. rev15) and the automated1 parameter. IQ-TREE (v.
197 2.2.0.3) was used to produce a consensus tree with 1000 bootstrap iterations using model test
198 results (Q.pgam+G4 model). The resulting tree was modified from iTOL (v.6) visualization.
199 Refer to Supplemental Methods/Results and Supplemental Tables for further details.

200

201 **Statistical analyses**

202 Comparisons of water column physiochemical features by ice cover were made in Prism
203 (v. 9.3.1) *via* two-tailed unpaired *t*-tests. Variability in expression (TPM) between transcriptomic
204 libraries was assessed *via* ANalysis Of Similarities (ANOSIM) and Similarity Percentage
205 (SIMPER) analyses using PRIMER (v.7) [55]. Bray-Curtis similarity and non-metric multi-
206 dimensional scaling (nMDS) were performed in R. Differential expression (DE) of transcript
207 abundance was performed using DESeq2 (v.1.28.1) [56]. Genes with an absolute \log_2 fold
208 change (Log_2FC) >2 and adjusted p-value of < 0.05 were considered differentially expressed. Z-
209 scores reported in heat maps were calculated by heatmap.ca (Clustering method: Average
210 linkage, Distance measurement method: Pearson) [57] using the DESeq2 variance stabilizing
211 transformed values (VST) [57]. Refer to Supplemental Methods/Results for further details.

212

213 **Results**

214 *Physiochemical profiles and winter community characterization*

215 Samples were collected across 12 sites throughout the central basin of Lake Erie with true
216 biological replication at a subset of stations (Figure 1C) (Supplemental Table 1). Temporally, the
217 samples span February-March 2019 and February-June 2020, yielding 14 winter and 6 spring
218 libraries. Climatically, the winter of 2019 was a year of high ice cover (mean maximum ice cover
219 of 80.9%), whereas winter 2020 was a year of negligible ice cover (mean maximum ice cover of
220 19.5%) [58] (Figure 1D). Libraries 1-4 were collected during ice cover (ranging from 3-15 cm in
221 thickness) while winter libraries 5-14 were collected during ice-free conditions. Winter lake
222 surface temperatures ranged from \sim 0-6 °C across sample sites (Supplemental Figure 1A).
223 Overall, nutrient concentrations at ice-covered sites were not significantly different from ice-free

224 sites save for nitrate (Supplemental Figure 1B-H). While not significant ($p \geq 0.13$), the highest
225 total Chl a concentrations ($> 0.22 \mu\text{m}$) coincided with ice cover (Figure 2A, B). The larger sized-
226 fraction of phytoplankton contributed an average of 70% (+/- 27%) to total Chl a during ice
227 cover and 50% (+/- 13%) in ice-free winter sites (Supplemental Figure 2), but the differences
228 were not significant ($p = 0.22$). Cell concentrations of diatoms (Bacillariophyta) dominated the
229 winter water column regardless of ice conditions, with other eukaryotic phytoplankton (e.g.,
230 Chlorophyta, Cryptophyta, and Dinophyta) present at concentrations 1-2 orders of magnitude
231 lower (Supplemental Figure 3). While Bacillariophyta concentrations decreased slightly at ice-
232 free sites ($p = 0.33$), Dinophyta concentrations significantly increased ($p = 0.03$), with
233 Cryptophyta and Chlorophyta exhibiting similar trends ($p \geq 0.05$). Overall, centric diatoms
234 (Mediophyceae, Coscinodiscophyceae) dominated the winter diatom community while pennate
235 diatoms (Bacillariophyceae, Fragilarophyceae) were found at concentrations an order of
236 magnitude lower (Figure 2C, D). Despite this dominance, centric diatoms demonstrated a
237 decreasing trend in ice-free samples while pennate diatoms exhibited significant increases in ice-
238 free samples ($p = 0.03$) albeit remaining at low abundances. Cell concentrations of the centric
239 bloom formers *Stephanodiscus* spp. and *A. islandica* were highest during ice cover (Figure 2E,
240 F). Notably, *Stephanodiscus* spp. concentrations were significantly higher than *A. islandica* in
241 ice-covered samples ($p = 0.03$), yet not significantly greater than *A. islandica* in ice-free samples
242 ($p = 0.19$) (Supplemental Figure 4). Further, while small centric diatoms (5-20 μm size) were not
243 detected in ice covered samples, they were found to range from ~300-3,000 cells L^{-1} in ice-free
244 samples (Supplemental Figure 5). These small centric diatom taxa accounted for ~83% of the
245 winter diatom community at site 8, although they otherwise contributed an average of 26% to the
246 total diatom community in ice-free samples (Supplemental Figure 6).

247

248 *Transcriptomic response of winter diatom community to ice cover*

249 Diatoms dominated the winter transcriptional pool across major eukaryotic

250 phytoplankton communities regardless of ice cover (Figure 3A). In turn, diatoms of the class

251 Mediophyceae dominated diatom community transcription regardless of ice cover (Figure 3B).

252 At the genus level of each class, there was a lack of definitive trends across libraries thus they

253 are omitted from the main text (Supplemental Figures 7-10). Overall, there was no correlation

254 between diatom cell abundance and transcript abundance (Supplemental Figure 11). Refer to

255 Supplemental Methods/Results and Supplemental Tables for further detail.

256 Normalized expression (TPM) profiles of the total water column community displayed

257 clustering by ice cover (Figure 4A), with SIMPER analyses demonstrating an average

258 dissimilarity of 64% between ice cover and ice-free winter libraries (Supplemental Table 1P).

259 ANOSIM tests confirmed ice strongly affected winter community gene expression ($R = 0.87$, $p =$

260 0.002) (Supplemental Figure 12A) (Supplemental Table 1Q). Surprisingly, diatom community

261 expression did not cluster as strongly by ice cover (Figure 4B), with SIMPER analyses indicating

262 an average dissimilarity of 47% between ice cover and ice-free libraries (Supplemental Table

263 1T). ANOSIM tests confirmed ice cover exerts a lesser influence on winter diatom community

264 expression overall compared to the full water column community ($R = 0.282$, $p = 0.059$)

265 (Supplemental Figure 12B). In contrast, season had a strong effect on diatom expression

266 (SIMPER Average dissimilarity = 77%; ANOSIM $R = 0.927$, $p = 0.001$) (Supplemental Tables

267 1V, W).

268 To investigate how ice cover contributed to the ~50% dissimilarity in winter diatom

269 expression, DE analyses were performed. These results indicated 354 genes belonging to

270 putative Bacillariophyta were differentially expressed ($|Log_2FC| \geq 2$, $p_{adj} < 0.05$), with 311 of
271 these genes increasing in relative expression in ice free samples (variable of interest) and 43
272 decreasing (Supplemental Table 1X). Diatoms of the class Mediophyceae had the highest
273 representation, comprising ~50% of DE genes while other classes formed a net total of ~10%
274 (40% unclassified diatoms) (Supplemental Figure 13A). Further analysis revealed 33% of the
275 polar centric DE genes were annotated as *Chaetoceros*-like (Supplemental Figure 13B), despite
276 *Chaetoceros*-like genes forming $\leq 10\%$ of mapped reads throughout the winter libraries
277 (Supplemental Figure 7). Here, the “*Chaetoceros*-like” label arises as the transcriptomes were
278 annotated with largely marine-comprised databases due to a lack of comprehensive freshwater
279 taxonomic sequencing [9, 59]. Hence, diatom class are reported in-text, genera are reported in
280 the Supplemental.

281 Genes categorized in COG category C (Energy production and conversion) were the
282 second highest represented category within the DE dataset, with most genes exhibiting increased
283 expression within ice-free diatom communities (Figure 5). Of these genes, 64% belonged to the
284 class Mediophyceae (Figure 5A, Supplemental Figure 14). Notably, the expression of genes
285 encoding for iron-containing photosynthetic proteins such (ferrodoxin-*petF*, flavoprotein-*etfA*,
286 and ferritin-*ftnA*) increased in relative expression in ice-free communities while expression of
287 photosystem II-*psbA* decreased (Figure 5B, C). Likewise, relative expression of genes within
288 COG category P (Inorganic ion transport and metabolism) increased in ice-free samples
289 (Supplemental Figure 15 A,), with expression of putative iron transporting genes (OMFeT_1-3)
290 increasing in ice-free communities. DE genes within COG category P also largely belong to the
291 Mediophyceae class, comprising ~40% of the annotated genes (Supplemental Figure 15, 16).
292 Notably, two proton-pumping rhodopsin genes (PPRs. COG S), which were most recently found

293 to be a light-driven, retinal-based alternative to classical phototrophy in a cold-adapted
294 freshwater photosynthetic bacterium [60], significantly increased in expression within ice-free
295 diatom communities (Figure 6A, Supplemental Figure 17A). Further, the expression 9 additional
296 diatom PPRs increased within the ice-free water column, though they fell short of differential
297 expression (Supplemental Figure 17B). Taxonomic annotations demonstrated these 11 PPRs
298 largely belonged to the Fragilario phyceae (33.33%) and Mediophyceae (22.22%) classes
299 (Unclassified Diatoms = 44.44%), with the two DE PPRs annotated at the phylum (PPR_1,
300 Bacillariophyta) and genus level (PPR_2, *Pseudo-nitzschia fraudulenta*-like). Phylogenetic
301 analyses suggested diatoms horizontally acquired PPRs from bacteria, as there is evidence for at
302 least 3 instances of horizontal gene transfer within our analysis (Figure 6C). The majority of the
303 PPRs in our study clustered with or near Eukaryotic rhodopsins. Notably, the most highly DE
304 PPR in our study (PPR_2, gene 538736) clustered closely with the marine diatom PPR belonging
305 to *Psuedo nitzschia granii* (Figure 6C) [61, 62]. Refer to Supplemental Methods/Results and
306 Supplemental Tables for further details.

307 DE analyses in response to season were performed with diatom libraries to identify trends
308 truly unique to the ice cover DE dataset. The top 10 COG categories represented in each dataset
309 overlapped except for COG category M, which was the third most abundant in ice cover analyses
310 compared to the twelfth most abundant in season analyses (Supplemental Figure 18). Further
311 analysis of these COG M (Cell wall, membrane, and envelope biogenesis) genes revealed 58%
312 belonged to the class Mediophyceae (Figure 7A, Supplemental Figure 19). Intriguingly, 50% of
313 the DE COG M genes encode for fasciclins (FAS1) which increased in expression under ice-free
314 conditions (Figure 7B, C). Fasciclins are secreted glycoproteins involved in diatom cell-cell
315 adhesion and cell-extracellular matrix adhesion [63, 64]. All 18 DE fasciclin genes were either

316 assigned to the class Mediophyceae or unclassified beyond the phylum level (Bacillariophyta).
317 Phylogenetic analyses indicated diatoms horizontally acquired FAS1 from bacteria, as there is
318 evidence for at least 6 instances of horizontal gene transfer within our analysis (Figure 7D).
319 Broadly, the FAS1 domain is widely distributed in diatoms, with ~140 marine and freshwater
320 diatoms found to contain this protein domain including the model cold-adapted diatom
321 *Fragilaropsis cylindrus* [65]. Refer to Supplemental Methods/Results and Supplemental Tables
322 for further details.

323

324 **Discussion**

325 The present study examined how phytoplankton (specifically diatoms) are responding to
326 rapidly declining ice cover in a northern temperate lake (Lake Erie). Indeed, ice cover has
327 declined by ~70% on the Laurentian Great Lakes over the 45-year period from 1973-2017 [66].
328 Notably, it has been suggested this decline in ice cover increases light limitation in shallow lakes
329 such as Lake Erie, hence we investigated this hypothesis that diatoms are light limited in the
330 turbid ice-free water column [4]. In this study, we demonstrated ice-free conditions decreased
331 diatom bloom magnitude and altered composition. Notably, diatoms exhibited increased relative
332 expression of photosynthesis and iron-transport genes under ice-free conditions: trends which are
333 consistent with light limitation [67, 68]. Further, metatranscriptomic analysis provides evidence
334 for two novel hypotheses concerning diatom adaptations to the ice free state of the lake: (1) *The*
335 *ice cover PPR energy hypothesis* and (2) *The fasciclin mediated rafting hypothesis*. We provide
336 this information couched within the context of the ecophysiological implications of a climatically
337 altered future for psychrophilic aquatic communities.

338

339 **Ice free conditions alter diatom bloom magnitude and composition**

340 It was previously noted *A. islandica* biovolumes were 95% decreased in the ice-free
341 turbid water column (2012) compared to ice-covered conditions the years prior (2010, 2011);
342 with light limitation cited as the potential driver of this trend [4]. By comparison, Chl *a* biomass,
343 centric diatom counts, and *A. islandica* counts did not significantly decrease relative to ice cover
344 in our study, though they all exhibited a consistent declining trend. However, our findings are in
345 juxtaposition to a prior Lake Erie winter study (2007-2010) which reported abundances of *A.*
346 *islandica* and *Stephanodiscus* spp. 1-2 magnitudes higher, with Chl *a* concentrations supporting
347 this trend [3]. In addition, subsequent studies also reported diatom communities overwhelmingly
348 dominated by *A. islandica*, with *Stephanodiscus* spp. present in lesser concentrations [3, 9-11,
349 69]. In contrast, we discovered cell abundances of *Stephanodiscus* spp. were significantly higher
350 than *A. islandica* in the ice-covered community. We hypothesize a decrease in consecutive years
351 of high ice cover may drive this decline of *A. islandica* dominance (Figure 1D). Regardless, our
352 results indicate the winter diatom bloom community has markedly declined in magnitude and
353 altered in composition since prior winter Lake Erie surveys (2007-2012).

354 In turn, it has been suggested that declines in diatom biomass may cause this niche to be
355 filled by cryptophytes and dinoflagellates, as mixotrophs are suggested to be better suited for the
356 turbid water column [4, 7]. While we observed significantly higher abundances of these groups
357 in ice-free samples within our study, their cellular and transcriptional abundances remained
358 below centric diatoms by an order of magnitude. Hence, our results demonstrate that low ice
359 cover during this season did not induce significant large-scale phyla-level shifts in major
360 eukaryotic phytoplankton community composition as previously suggested. Cumulatively, this

361 implies future ice-free winter communities may remain dominated by centric diatoms as
362 observed in this study, albeit at a lesser magnitude.

363 While net centric diatom abundances did not significantly differ by ice conditions in our
364 study, diatom community composition exhibited significant changes at the genus level. Cell
365 abundances of *Stephanodiscus* spp., were ~50% lower in ice-free samples, resulting in ~equal
366 abundances of *Stephanodiscus* spp. and *A. islandica* within the ice-free water column. Further,
367 small centric diatom taxa (5-20 μm size) were mainly absent in samples from ice-covered sites
368 yet formed 10-82% of total diatom counts in ice-free sites, with a bloom of these taxa noted at
369 site 8. This suggests ice-free conditions may increase populations of smaller, centric diatoms in
370 future warmer and ice-free winters. The trend is supported by prior studies which demonstrate
371 warming temperatures decrease phytoplankton cell size [70] and select for smaller taxa [71, 72].
372 We also noted significant increases in pennate diatom abundance in the ice-free water column.
373 Cumulatively, if these observations represent long-term trends, future ice-free diatom
374 communities will be more diverse with lower biomass.

375

376 **Evidence of light limitation within the ice-free water column**

377 The relative expression of photosynthesis-associated genes increased overall within ice-
378 free diatom communities, suggesting potential efforts to increase light capture and light-driven
379 processes within the turbid water column. Most notably, we observed an increase in expression
380 of iron transporters coinciding with various genes encoding for iron-rich photosynthetic
381 structures and photosystem components. In support, a prior study found temperate phytoplankton
382 acclimate to low light conditions by increasing their number of iron-rich photosystems [68].
383 Thus, our data suggest freshwater diatoms in the ice-free, turbid Lake Erie water column were

384 attempting to build additional photosystems in response to decreased light availability. Indeed,
385 our data offers transcriptional support for a prior study which found primary production rates
386 (measured via C¹⁴ tracing) to be lower within the Lake Erie ice-free water column (2012)
387 compared to the ice covered water column (2010-2011) [4]. Further, two diatom PPRs within our
388 dataset increased within the ice-free water column while *psbA* coincidentally decreased,
389 suggesting diatoms may be attempting to use alternative phototrophic strategies other than
390 classical photosynthesis within the ice-free water column. Cumulatively, this suggests diatoms
391 may be attempting to use alternative light-driven energy mechanisms as a means to evade
392 classical light limitation. Other studies demonstrate enlarged light antennae is another response
393 to light limitation, as this increases light harvesting [73] and is suggested to be particularly
394 advantageous in cold environments [67]. While we did not observe evidence of this phenomenon
395 in our dataset, this may have occurred prior or post-sampling of the community as
396 metatranscriptomics offers only a “snapshot” episodic glimpse at community response. Hence,
397 while we found supportive evidence of light limitation in this study, further research is required
398 in seasonally cold temperate systems.

399

400 **The role of PPRs as a function of ice cover**

401 We observed increases in the expression of genes encoding for PPRs within the ice-free
402 diatom community. PPRs are light-harvesting retinal-containing proton pumps distinct from the
403 chlorophyll-containing antenna of classical photosynthesis [74], yet capable of absorbing as
404 much light energy as Chl *a* [75]. On a global scale, it is thought microbial rhodopsin driven
405 phototrophy is a major marine light harvesting process [76]. Beyond prokaryotes, they have been
406 characterized within a number of marine diatoms [62] and dinoflagellates [77]. Notably, PPRs

407 have been suggested to serve as an alternative light-driven energy source for marine diatoms
408 under conditions which limit classical photosynthesis [62, 78]. However, compared to the marine
409 literature [75, 79-83], PPRs are widely understudied in fresh waters. To our knowledge, this
410 study is the first to report the presence of PPRs within freshwater diatoms to date;—although we
411 are not the first to suggest PPRs may play a role in energy generation beneath ice. It was recently
412 found that a photoheterotrophic bacterium isolated from an alpine lake used PPRs as an
413 alternative phototrophy mechanism [60]. The authors of this study further hypothesized the
414 contribution of PPRs to energy generation is linked to ice cover. Here, we present evidence
415 diatoms within the ice-free Lake Erie water column increase the expression of PPRs in the ice-
416 free, low- light turbid environment, which lends support to this hypothesis regarding an
417 ecophysiological role of PPRs within icy freshwater environments.

418 Nonetheless, there are a variety of ecophysiological explanations for this PPR
419 phenomenon. This may be an attempt to scavenge wavelengths of light beyond those absorbed
420 by Chl *a*; lending further evidence they are light limited. Indeed, PPRs absorb at a maximum
421 wavelength of ~525nm (green light) [83] in contrast to Chl *a* which absorbs at a 430-470nm
422 (blue) and 660-670nm (red). Hence, PPRs would allow diatoms to access alterative light niches
423 in the turbid water column. This is further supported in our data, as expression of two diatom
424 PPRs was significantly higher in the ice-free water column whereas the expression of *psbA* was
425 significantly higher in ice-covered samples (Figure 6A). Alternatively, green light penetrates up
426 to 100m depth, with only to blue light penetrating further. Hence, PPRs may be involved in light-
427 acquisition during well-mixed isothermal conditions when diatoms would be mixing throughout
428 the benthic and pelagic environments in shallow lakes (Supplemental Figure 20). Broadly, this
429 suggests an ecophysiological role of PPRs for diatoms across global freshwater and marine

430 environments. Thus, our observations suggest that the role of these proton-pumping rhodopsins
431 within fresh waters demands more attention [84], as it is possible that in future scenarios (less ice
432 cover, more turbidity) they may serve as important evolutionary selectors.

433

434 **The role of fasciclins in the ice-free turbid water column**

435 Though fasciclins (FAS1) remain widely uncharacterized in diatoms, prior studies have
436 described fasciclins within the diatom species *Amphora coffeaeformis* [64] and *Phaeodactylum*
437 *tricornutum* [63]. Both studies identified fasciclin proteins within diatom-secreted exopolymer
438 substance adhesion trails and concluded these molecules facilitate diatom motility, adhesion, and
439 aggregation. In this study, 58% of the DE diatom fasciclins belonged to the class Mediophyceae
440 (27% to unclassified diatoms). As a result, we hypothesize Mediophyceae diatoms were rafting
441 via cell-adhesion fasciclins to optimize their location within the ice-free, turbid Lake Erie water
442 column, thus avoiding light limitation.

443 This hypothesis is largely based on a similar “rafting” strategy that is well-documented in
444 centric marine diatoms, notably *Rhizosolenia* spp. [85-88]. These studies demonstrated rafts
445 become positively buoyant in response to a variety of physiological stressors, including iron
446 limitation [86, 89, 90]. Further, our phylogenetic analyses demonstrated this fasciclin-mediated
447 rafting hypothesis may not be unique to Lake Erie diatoms alone. Fasciclins were identified in
448 ~140 marine and freshwater diatoms including the model polar marine diatom *Fragilariopsis*
449 *cylindrus* [91]. Hence, this further implies an ecophysiological role exists for these proteins in
450 the globally frigid waters. In turn, this also indicates further research is required regarding the
451 role of fasciclins within polar aquatic systems and psychrophilic organisms broadly, especially
452 when considering the rapid global decline in ice cover.

453

454 **Conclusions**

455 Lakes are sentinels of climate change [92]. Indeed, our study builds on data which
456 demonstrate community-wide responses to climate-driven declines in ice cover are already
457 underway. Notably, we provide evidence which suggests diatom declines are driven by light-
458 limitation in the turbid ice-free water column (Figure8). Indeed, Ozersky et al., [7] suggested
459 warmer winters will induce a change in the Great Lakes mixing regime, shifting from dimictic
460 mixing patterns to a warm monomictic mixing pattern characterized by continuous isothermal
461 conditions throughout winter. Hence, adaptations to evade coinciding exacerbations in light
462 limitation (such as the possession of PPRs and FAS1 described in this study) may be of increased
463 importance in future winter diatom survival as phytoplankton adapt to ice-free winters. Indeed,
464 our data suggests climate change may not be just a “temperature” problem in the case of shallow
465 temperate lakes, but a “light” problem. Regardless, with diatoms previously described as “one of
466 the most rapidly evolving eukaryotic taxa on Earth” [93, 94] and prone to promiscuous
467 horizontal gene transfer events [95], it would be surprising if they failed to adapt to an ice-free
468 future. Ultimately, we cannot place the consequences of the metatranscriptomic observations we
469 describe in a quantitative framework. To this end, our observations, which demonstrate
470 variability associated with conditions consistent with projected future climate scenarios, carve
471 out a critical path forward and provide cautionary insight of what may be yet to come in global
472 temperate lakes.

473

474

475

476

477

478

479 **Data availability**

480 Raw and processed reads for the data used in this study are available through the JGI Data Portal
481 (<https://data.jgi.doe.gov>) under Proposal ID 503851.

482

483 **Conflict of Interest**

484 *The authors declare that the research was conducted in the absence of any commercial or*
485 *financial relationships that could be construed as a potential conflict of interest.*

486

487 **Author Contributions**

488 This project was designed by SW and RMLM. Samples were collected by RMLM, TF, GB, and
489 JC. Phytoplankton enumeration and identification was performed by WC. RNA extractions in
490 addition to quality/quantity assessment were performed by BZ. Metatranscriptomic processing
491 was performed by BZ, NG, EC and LD using a pipeline established by NG. Python scripts
492 associated with metatranscriptomic pipeline were written by AT. The phylogenetic tree and
493 corresponding analyses were performed by EC. Statistical analyses were made by BZ. Figures
494 and the first full draft were made by BZ. All authors contributed to the revisions and final
495 version of the manuscript.

496

497 **Acknowledgements**

498 We are grateful to the command and members of the U.S. Coast Guard Cutter Neah Bay,
499 Canadian Coast Guard Ship *Limnos* and M/V *Orange Apex* for their help with sample collection
500 and the generation of hydrochemistry data. We thank Daniel H. Peck, James T. Anderson, Derek
501 Niles and Arthur Zastepa for their help with sample collection and pre-processing. We thank
502 Christa Pennacchio with the JGI for her coordination and sequencing expertise. We thank Dr.
503 Gary LeCleir, Katelyn Houghton, Dr. Erik Zinser, and Dr. Jill Mikucki for their comments and
504 suggestions. This work was funded by the National Institutes of Health, NIEHS grant
505 1P01ES023-28939-01, National Science Foundation grant OCE-1840715 (GB, RMLM, JC,
506 SW), NSERC grant RGPN-2019-03943 (RMLM) and funding from the NSF GRFP DGE-
507 19389092 (BNZ). This work conducted by the U.S. Department of Energy Joint Genome
508 Institute (<https://ror.org/04xm1d337>), a DOE Office of Science User Facility, is supported by the
509 Office of Science of the U.S. Department of Energy operated under Contract No. DE-AC02-
510 05CH11231.”

511

512 **Additional Information**

513 **Supplementary information** is electronically available at XXXXX.

514

515 **Correspondence** and requests for materials should be addressed to Steven W. Wilhelm or R.
516 Michael L. McKay.

517

518 **Reprints and permission information** is available at <http://www.nature.com/reprints>.

519

520

521

522

523 **References**

- 524 1. Sommer, U., et al., *The PEG-model of seasonal succession of planktonic events in fresh waters.*
525 Archiv für Hydrobiologie, 1986. **106**(4): p. 433-471.
- 526 2. Sommer, U., et al., *Beyond the Plankton Ecology Group (PEG) model: mechanisms driving*
527 *plankton succession.* Annual Review of Ecology, Evolution and Systematics, 2012. **43**: p. 429-448.
- 528 3. Twiss, M., et al., *Diatoms abound in ice-covered Lake Erie: An investigation of offshore winter*
529 *limnology in Lake Erie over the period 2007 to 2010.* Journal of Great Lakes Research, 2012.
530 **38**(1): p. 18-30.
- 531 4. Beall, B., et al., *Ice cover extent drives phytoplankton and bacterial community structure in a*
532 *large north-temperate lake: implications for a warming climate.* Environmental Microbiology,
533 2016. **18**(6): p. 1704-1719.
- 534 5. Powers, S.M. and S.E. Hampton, *Winter limnology as a new frontier.* Limnology and
535 Oceanography Bulletin, 2016. **25**(4): p. 103-108.
- 536 6. Hampton, S.E., et al., *Ecology under lake ice.* Ecology letters, 2017. **20**(1): p. 98-111.
- 537 7. Ozersky, T., et al., *The changing face of winter: lessons and questions from the Laurentian Great*
538 *Lakes.* 2021, Wiley Online Library: Journal of Geophysical Research: Biogeosciences.
- 539 8. D'souza, N.A., *Psychrophilic diatoms in ice-covered Lake Erie.* 2012, Bowling Green State
540 University.
- 541 9. Edgar, R., et al., *Adaptations to photoautotrophy associated with seasonal ice cover in a large*
542 *lake revealed by metatranscriptome analysis of a winter diatom bloom.* Journal of Great Lakes
543 Research, 2016. **42**(5): p. 1007-1015.
- 544 10. Wilhelm, S.W., et al., *Seasonal changes in microbial community structure and activity imply*
545 *winter production is linked to summer hypoxia in a large lake.* FEMS Microbiology Ecology, 2014.
546 **87**(2): p. 475-485.
- 547 11. Saxton, M.A., et al., *Seasonal Si: C ratios in Lake Erie diatoms—evidence of an active winter*
548 *diatom community.* Journal of Great Lakes Research, 2012. **38**(2): p. 206-211.
- 549 12. Reavie, E.D., et al., *Winter–spring diatom production in Lake Erie is an important driver of*
550 *summer hypoxia.* Journal of Great Lakes Research, 2016. **42**(3): p. 608-618.
- 551 13. Kong, X., et al., *Unravelling winter diatom blooms in temperate lakes using high frequency data*
552 *and ecological modeling.* Water Research, 2021. **190**: p. 116681.
- 553 14. Katz, S.L., et al., *The “M. elosira years” of Lake Baikal: Winter environmental conditions at ice*
554 *onset predict under-ice algal blooms in spring.* Limnology and Oceanography, 2015. **60**(6): p.
555 1950-1964.
- 556 15. Izmost'eva, L.R., et al., *Seasonal dynamics of common phytoplankton in Lake Baikal.* Proc.
557 Russian Acad. Sci. Sci. Centre, 2006. **8**: p. 191-196.
- 558 16. Spaulding, S. and J. Baron, *Winter phytoplankton dynamics in a subalpine lake, Colorado, USA.*
559 Archiv für Hydrobiologie, 1993: p. 179-198.
- 560 17. Petrova, N.A., *Seasonality of Melosira-plankton of the great northern lakes.* Hydrobiologia, 1986.
561 **138**: p. 65-73.
- 562 18. Arai, H. and T. Fukushima. *Impacts of long-term increase in silicon concentration on diatom*
563 *blooms in Lake Kasumigaura, Japan.* in *Annales de Limnologie-International Journal of*
564 *Limnology.* 2014. EDP Sciences.
- 565 19. Kiss, K. and S. Genkal. *Winter blooms of centric diatoms in the River Danube and in its side-arms*
566 *near Budapest (Hungary).* in *Twelfth International Diatom Symposium: Proceedings of the*
567 *Twelfth International Diatom Symposium, Renesse, The Netherlands, 30 August–5 September*
568 *1992.* 1993. Springer.
- 569 20. D'souza, N., et al., *Diatom assemblages promote ice formation in large lakes.* The ISME Journal,
570 2013. **7**(8): p. 1632-1640.

571 21. Nelson, D.M., et al., *Production and dissolution of biogenic silica in the ocean: revised global*
572 *estimates, comparison with regional data and relationship to biogenic sedimentation*. Global
573 Biogeochemical Cycles, 1995. **9**(3): p. 359-372.

574 22. Rühland, K.M., A.M. Paterson, and J.P. Smol, *Lake diatom responses to warming: reviewing the*
575 *evidence*. Journal of Paleolimnology, 2015. **54**(1): p. 1-35.

576 23. Struyf, E., et al., *The global biogeochemical silicon cycle*. Silicon, 2009. **1**(4): p. 207-213.

577 24. Benoiston, A.-S., et al., *The evolution of diatoms and their biogeochemical functions*.
578 Philosophical Transactions of the Royal Society B: Biological Sciences, 2017. **372**(1728): p.
579 20160397.

580 25. Wang, J., et al., *Decadal variability of Great Lakes ice cover in response to AMO and PDO, 1963–*
581 *2017*. Journal of Climate, 2018. **31**(18): p. 7249-7268.

582 26. Mason, L.A., et al., *Fine-scale spatial variation in ice cover and surface temperature trends across*
583 *the surface of the Laurentian Great Lakes*. Climatic Change, 2016. **138**: p. 71-83.

584 27. Filazzola, A., et al., *Climate change drives increases in extreme events for lake ice in the Northern*
585 *Hemisphere*. Geophysical Research Letters, 2020. **47**(18): p. e2020GL089608.

586 28. Bolsenga, S. and H. Vanderploeg, *Estimating photosynthetically available radiation into open*
587 *and ice-covered freshwater lakes from surface characteristics; a high transmittance case study*.
588 Hydrobiologia, 1992. **243**: p. 95-104.

589 29. Chandler, D.C., *Limnological studies of western Lake Erie IV. Relation of limnological and climatic*
590 *factors to the phytoplankton of 1941*. Transactions of the American Microscopical Society, 1944.
591 **63**(3): p. 203-236.

592 30. Valipour, R., et al., *Sediment resuspension mechanisms and their contributions to high-turbidity*
593 *events in a large lake*. Limnology and Oceanography, 2017. **62**(3): p. 1045-1065.

594 31. Vanderploeg, H.A., et al., *Plankton ecology in an ice-covered bay of Lake Michigan: Utilization of*
595 *a winter phytoplankton bloom by reproducing copepods*. Hydrobiologia, 1992. **243**: p. 175-183.

596 32. Vanderploeg, H., et al., *Anatomy of the recurrent coastal sediment plume in Lake Michigan and*
597 *its impacts on light climate, nutrients, and plankton*. Journal of Geophysical Research: Oceans,
598 2007. **112**(C3).

599 33. McKay, R.M.L., et al., *Winter limnology on the Great Lakes: The role of the US Coast Guard*.
600 Journal of Great Lakes Research, 2011. **37**(1): p. 207-210.

601 34. Zepernick, B.N., et al., *Metatranscriptomic Sequencing of Winter and Spring Planktonic*
602 *Communities from Lake Erie, a Laurentian Great Lake*. Microbiology Resource Announcements,
603 2022: p. e00351-22.

604 35. Bullerjahn, G.S., J.T. Anderson, and R.M. McKay, *Winter survey data from Lake Erie from 2018–*
605 *2020*. 2022: Biological and Chemical Oceanography Data Management Office (BCO-DMO).

606 36. Martin, R.M. and S.W. Wilhelm, *Phenol-based RNA Extraction from Polycarbonate Filters*.
607 protocols.io, 2020.

608 37. Clum, A., et al., *DOE JGI metagenome workflow*. Msystems, 2021. **6**(3): p. e00804-20.

609 38. Bushnell, B., *BBMap: a fast, accurate, splice-aware aligner*. 2014, Lawrence Berkeley National
610 Lab.(LBNL), Berkeley, CA (United States).

611 39. Gilbert, N.E., et al., *Bioavailable iron titrations reveal oceanic Synechococcus ecotypes optimized*
612 *for different iron availabilities*. ISME Communications, 2022. **2**(1): p. 1-12.

613 40. Li, D., et al., *MEGAHIT v1. 0: a fast and scalable metagenome assembler driven by advanced*
614 *methodologies and community practices*. Methods, 2016. **102**: p. 3-11.

615 41. Gurevich, A., et al., *QUAST: quality assessment tool for genome assemblies*. Bioinformatics,
616 2013. **29**(8): p. 1072-1075.

617 42. Zhu, W., A. Lomsadze, and M. Borodovsky, *Ab initio gene identification in metagenomic*
618 *sequences*. Nucleic Acids Research, 2010. **38**(12): p. e132-e132.

619 43. Krinos, A.I., et al., *EUKulele: Taxonomic annotation of the unsung eukaryotic microbes*. arXiv
620 preprint arXiv:2011.00089, 2020.

621 44. Reavie, E., *Asymmetric, biraphid diatoms from the Laurentian Great Lakes*. PeerJ Aquatic
622 Biology, 2023.

623 45. Cantalapiedra, C.P., et al., *eggNOG-mapper v2: functional annotation, orthology assignments,*
624 *and domain prediction at the metagenomic scale*. Molecular Biology and Evolution, 2021.
625 **38**(12): p. 5825-5829.

626 46. Liao, Y., G.K. Smyth, and W. Shi, *featureCounts: an efficient general purpose program for*
627 *assigning sequence reads to genomic features*. Bioinformatics, 2014. **30**(7): p. 923-930.

628 47. Wheeler, D.L., et al., *Database resources of the national center for biotechnology information*.
629 Nucleic Acids Research, 2007. **35**(suppl_1): p. D5-D12.

630 48. Buchfink, B., C. Xie, and D.H. Huson, *Fast and sensitive protein alignment using DIAMOND*.
631 Nature Methods, 2015. **12**(1): p. 59-60.

632 49. Fu, L., et al., *CD-HIT: accelerated for clustering the next-generation sequencing data*.
633 Bioinformatics, 2012. **28**(23): p. 3150-3152.

634 50. Katoh, K. and D.M. Standley, *MAFFT multiple sequence alignment software version 7:*
635 *improvements in performance and usability*. Molecular Biology and Evolution, 2013. **30**(4): p.
636 772-780.

637 51. Capella-Gutiérrez, S., J.M. Silla-Martínez, and T. Gabaldón, *trimAl: a tool for automated*
638 *alignment trimming in large-scale phylogenetic analyses*. Bioinformatics, 2009. **25**(15): p. 1972-
639 1973.

640 52. Larsson, A., *AliView: a fast and lightweight alignment viewer and editor for large datasets*.
641 Bioinformatics, 2014. **30**(22): p. 3276-3278.

642 53. El-Gebali, S., et al., *The Pfam protein families database in 2019*. Nucleic Acids Research, 2019.
643 **47**(D1): p. D427-D432.

644 54. Letunic, I. and P. Bork, *Interactive Tree Of Life (iTOL) v4: recent updates and new developments*.
645 Nucleic Acids Research, 2019. **47**(W1): p. W256-W259.

646 55. Clarke, K. and R. Gorley, *Getting started with PRIMER v7*. PRIMER-E: Plymouth, Plymouth Marine
647 Laboratory, 2015. **20**.

648 56. Love, M.I., W. Huber, and S. Anders, *Moderated estimation of fold change and dispersion for*
649 *RNA-seq data with DESeq2*. Genome Biology, 2014. **15**(12): p. 1-21.

650 57. Babicki, S., et al., *Heatmapper: web-enabled heat mapping for all*. Nucleic Acids Research, 2016.
651 **44**(W1): p. W147-W153.

652 58. NOAA NOAA projects 30% maximum Great Lakes ice cover for winter. 2021.

653 59. Zepernick, B.N., et al., *Draft Genome Sequence of the Freshwater Diatom *Fragilaria crotonensis**
654 *SAG 28.96*. Microbiology Resource Announcements, 2022: p. e00289-22.

655 60. Kopejtka, K., et al., *A bacterium from a mountain lake harvests light using both proton-pumping*
656 *xanthorhodopsins and bacteriochlorophyll-based photosystems*. Proceedings of the National
657 Academy of Sciences, 2022. **119**(50): p. e2211018119.

658 61. Yoshizawa, S., et al., *Light-driven Proton Pumps as a Potential Regulator for Carbon Fixation in*
659 *Marine Diatoms*. Microbes and Environments, 2023. **38**(2): p. ME23015.

660 62. Marchetti, A., et al., *Marine diatom proteorhodopsins and their potential role in coping with low*
661 *iron availability*. The ISME Journal, 2015. **9**(12): p. 2745-2748.

662 63. Willis, A., et al., *Adhesion molecules from the diatom *Phaeodactylum tricornutum**
663 *(Bacillariophyceae): genomic identification by amino-acid profiling and in vivo analysis*. Journal
664 of Phycology, 2014. **50**(5): p. 837-849.

665 64. Lachnit, M., et al., *Identification of proteins in the adhesive trails of the diatom *Amphora**
666 *coffeaeformis*. Philosophical Transactions of the Royal Society B, 2019. **374**(1784): p. 20190196.

667 65. Otte, A., et al., *The diatom Fragilariopsis cylindrus: A model alga to understand cold-adapted life*.
668 *Journal of Phycology*, 2023.

669 66. Wang, J., et al., *Great Lakes ice climatology update of winters 2012-2017: Seasonal cycle, interannual variability, decadal variability, and trend for the period 1973-2017*. 2017.

670 67. Strzepek, R.F., P.W. Boyd, and W.G. Sunda, *Photosynthetic adaptation to low iron, light, and temperature in Southern Ocean phytoplankton*. *Proceedings of the National Academy of Sciences*, 2019. **116**(10): p. 4388-4393.

671 68. Suggett, D.J., et al., *Different strategies of photoacclimation by two strains of Emiliania huxleyi (Haptophyta)* 1. *Journal of Phycology*, 2007. **43**(6): p. 1209-1222.

672 69. Twiss, M.R., et al., *Phytoplankton growth dynamics in offshore Lake Erie during mid-winter*. *Journal of Great Lakes Research*, 2014. **40**(2): p. 449-454.

673 70. Bramburger, A.J., et al., *Decreases in diatom cell size during the 20th century in the Laurentian Great Lakes: a response to warming waters?* *Journal of Plankton Research*, 2017. **39**(2): p. 199-210.

674 71. Daufresne, M., K. Lengfellner, and U. Sommer, *Global warming benefits the small in aquatic ecosystems*. *Proceedings of the National Academy of Sciences*, 2009. **106**(31): p. 12788-12793.

675 72. Winder, M., J.E. Reuter, and S.G. Schladow, *Lake warming favours small-sized planktonic diatom species*. *Proceedings of the Royal Society B: Biological Sciences*, 2009. **276**(1656): p. 427-435.

676 73. Falkowski, P. and J. Raven, *Aquatic photosynthesis*, 2nd edn Princeton. 2007, NJ: Princeton University Press.[Google Scholar].

677 74. Yoshizawa, S., et al., *Proton-pumping rhodopsins in marine diatoms*. bioRxiv, 2022.

678 75. Gómez-Consarnau, L., et al., *Microbial rhodopsins are major contributors to the solar energy captured in the sea*. *Science Advances*, 2019. **5**(8): p. eaaw8855.

679 76. Gomez-Consarnau, L., et al., *Microbial rhodopsins are major contributors to the solar energy captured in the sea*. *Sciecne Advances*, 2019. **5**(8): p. eaaw8855.

680 77. Slamovits, C.H., et al., *A bacterial proteorhodopsin proton pump in marine eukaryotes*. *Nature Communications*, 2011. **2**: p. 183.

681 78. Marchetti, A., et al., *Comparative metatranscriptomics identifies molecular bases for the physiological responses of phytoplankton to varying iron availability*. *Proceedings of the National Academy of Sciences*, 2012. **109**(6): p. E317-E325.

682 79. Slamovits, C.H., et al., *A bacterial proteorhodopsin proton pump in marine eukaryotes*. *Nature communications*, 2011. **2**(1): p. 1-7.

683 80. Kwon, Y.M., et al., *Diversity and functional analysis of light-driven pumping rhodopsins in marine Flavobacteria*. *MicrobiologyOpen*, 2016. **5**(2): p. 212-223.

684 81. Hassanzadeh, B., et al., *Microbial rhodopsins are increasingly favoured over chlorophyll in High Nutrient Low Chlorophyll waters*. *Environmental Microbiology Reports*, 2021. **13**(3): p. 401-406.

685 82. Béja, O., et al., *Bacterial rhodopsin: evidence for a new type of phototrophy in the sea*. *Science*, 2000. **289**(5486): p. 1902-1906.

686 83. Béja, O., et al., *Proteorhodopsin phototrophy in the ocean*. *Nature*, 2001. **411**(6839): p. 786-789.

687 84. Sharma, A.K., et al., *Actinorhodopsin genes discovered in diverse freshwater habitats and among cultivated freshwater Actinobacteria*. *The ISME journal*, 2009. **3**(6): p. 726-737.

688 85. Villareal, T.A., M.A. Altabet, and K. Culver-Rymsza, *Nitrogen transport by vertically migrating diatom mats in the North Pacific Ocean*. *Nature*, 1993. **363**(6431): p. 709-712.

689 86. Villareal, T.A., et al., *Vertical migration of Rhizosolenia mats and their significance to NO_3^- fluxes in the central North Pacific gyre*. *Journal of Plankton Research*, 1996. **18**(7): p. 1103-1121.

690 87. Villareal, T.A., et al., *Upward transport of oceanic nitrate by migrating diatom mats*. *Nature*, 1999. **397**(6718): p. 423-425.

714 88. Villareal, T.A. and F. Lipschultz, *Internal nitrate concentrations in single cells of large*
715 *phytoplankton from the sargasso sea*. Journal of Phycology, 1995. **31**(5): p. 689-696.

716 89. McKay, R.M.L., T.A. Villareal, and J. La Roche, *Vertical migration by Rhizosolenia spp.*
717 *(Bacillariophyceae): Implications for Fe acquisition*. Journal of Phycology, 2000. **36**(4): p. 669-
718 674.

719 90. Villareal, T.A., unpublished.

720 91. Otte, A., et al., *The diatom Fragilaropsis cylindrus: A model alga to understand cold-adapted life*.
721 Journal of Phycology, 2023.

722 92. Adrian, R., et al., *Lakes as sentinels of climate change*. Limnology and oceanography, 2009.
723 **54**(6part2): p. 2283-2297.

724 93. Vardi, A., et al., *Diatom genomes come of age*. Genome Biology, 2009. **9**(12): p. 245.

725 94. Oliver, M.J., et al., *The mode and tempo of genome size evolution in eukaryotes*. Genome
726 Research, 2007. **17**(5): p. 594-601.

727 95. Dorrell, R.G., et al., *Phylogenomic fingerprinting of tempo and functions of horizontal gene
728 transfer within ochrophytes*. Proceedings of the National Academy of Sciences, 2021. **118**(4): p.
729 e2009974118.

730 96. NOAA-GLERL. *Historical Ice Cover*. [cited 2023 2-12-2023]; Available from:
731 <https://www.glerl.noaa.gov/data/ice/#historical>

732

733 **Figure Legends**

734

735 **Figure 1: Climatic, spatial and temporal variability across Lake Erie samples.** (A) MODIS
736 satellite image (March 16th, 2014) depicting a large amount of ice cover across the Great Lakes.
737 During the winter of 2014, Lake Erie had a mean annual ice cover of ~80%. (B) MODIS satellite
738 image (February 12th, 2023) depicting a lack of ice cover across the Great Lakes. Sediment
739 plumes can be observed throughout Lake Erie. During the winter of 2023, Lake Erie had a mean
740 annual ice cover of ~8%. Photo Credit: NOAA GLERL/NOAA Great Lakes CoastWatchNode.
741 (C) Sample sites across Lake Erie visited throughout winter-spring 2019 and 2020. (D)
742 Historical trends in Lake Erie mean annual maximum ice cover (%). Open circles are years that
743 (to our knowledge) do not have peer-reviewed published planktonic survey data. Solid black
744 circles are years that were previously surveyed in prior published studies. Solid blue circles are
745 years sampled in this study. Figure adapted from data retrieved from NOAA GLERL database
746 [96].

747

748 **Figure 2: Characterization of biotic community across Lake Erie sample sites.** Samples are
749 organized on the x-axis by season (W = winter, S = spring) and year. Solid shapes indicate the
750 sample was collected during ice cover (2019) open shapes indicate the sample was collected
751 during no ice cover (2020). Ice cover samples are indicated by a blue asterisk. (A) Total Chl *a*
752 concentration of the whole water column community (i.e., >0.22 μm in size) ($\mu\text{g L}^{-1}$) (B) Chl *a*
753 concentration of the large size fractioned community (i.e., >20 μm in size) ($\mu\text{g L}^{-1}$). (C) Cell
754 abundances (Cells L^{-1}) of centric diatoms (*Stephanodiscus* spp. + *A. islandica* + Small centric
755 diatoms of 5-20 μm). (D) Cell abundances of pennate diatoms (*Fragilaria* spp. + *Asterionella*
756 *formosa* + *Nitzschia* spp.). (E) Cell abundances (Cells L^{-1}) of *Stephanodiscus* spp., Mediophyceae
757 class. (F) Cell abundances (Cells L^{-1}) of *A. islandica*, Coscinodiscophyceae class.

758

759 **Figure 3: Relative transcript abundance of major eukaryotic phytoplankton taxa and**
760 **diatom classes.** Libraries are listed in chronological order of sample date on x-axes, with
761 biological replicates joined by grey horizontal bars. Ice cover samples are indicated by a blue
762 asterisk. (A) Relative transcript abundance of MEPT. All groups which formed <5% of the total
763 mapped reads are included within “Other” (Amoebozoa, Hiliomonadea, Excavata, Rhizaria, NA).
764 (B) Relative transcript abundance of Bacillariophyta classes Mediophyceae,
765 Coscinodiscophyceae, Bacillariophyceae, Fragilarophyceae and unclassified diatoms.

766

767 **Figure 4: Similarity (Bray-Curtis) clustering of the 20 metatranscriptomic library**
768 **normalized expression values (TPM).** (A) nMDS of the entire water column community
769 expression, stress value = 0.0633. (B) nMDS of the Bacillariophyta community expression,
770 stress value= 0.0497. Samples are presented as follows: February = squares, March = triangles.
771 May = diamonds, June = circles. Blue indicates the sample was collected during the winter,
772 black indicates the sample was collected during the spring. Solid shapes indicate the sample was
773 collected during ice cover (2019) open shapes indicate the sample was collected during no ice
774 cover (2020).

775

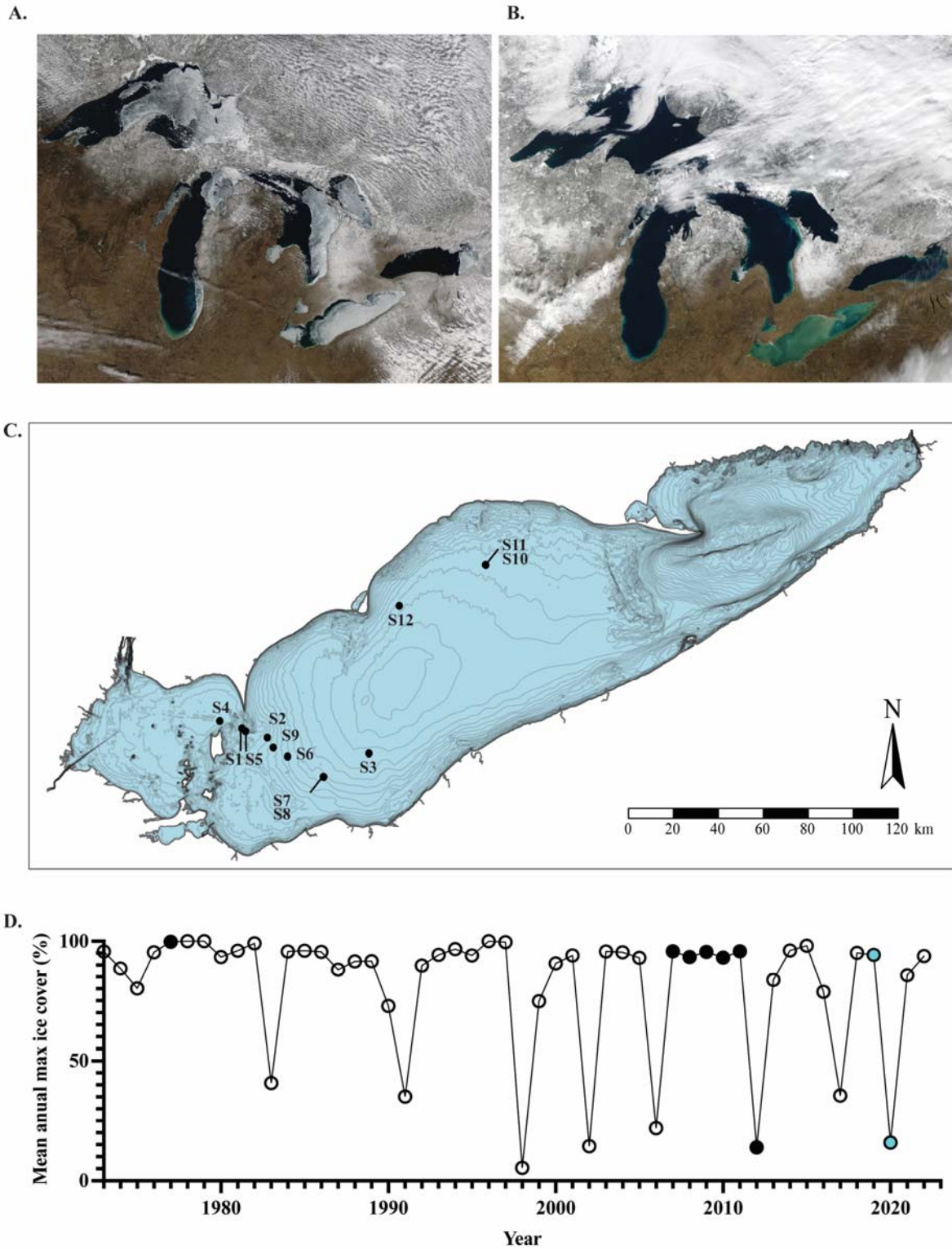
776 **Figure 5: Bacillariophyta energy production and conversion transcript abundance patterns**
777 **in response to ice cover.** A) Taxonomic distribution of DE genes categorized within COG
778 category C (Energy Production and Conversion). (B) COG assignments for all 354 DE genes in

779 response to ice cover, with COG category C indicated in blue. **(C)** Heatmap depicting COG
780 category C DE gene expression (VST) in response to ice cover across the 14 winter libraries.
781

782 **Figure 6: Bacillariophyta PPR transcript abundance patterns in response to ice. (A)**
783 Normalized expression (VST) of two DE genes functionally annotated as PPRs (PPR_1 (grey),
784 PPR_2 (teal)) and representative DE genes functionally annotated to be involved in photosynthesis
785 (black). Photosynthetic genes were selected because they are involved in light-harvesting (*psbA*,
786 *psbM*) or the transfer of electrons along the photosystems (*petF*). Each circle corresponds to gene
787 expression in one of the 14 libraries. Solid black circles indicate the sample was collected during
788 ice cover (2019) open shapes indicate the sample was collected during no ice cover (2020). **(B)**
789 Taxonomic distribution of the 11 genes functionally annotated as PPRs (and confirmed with
790 subsequent phylogenetic analysis). **(C)** Phylogenetic tree of PPR distribution within
791 diatoms. Study putative rhodopsin-like proteins (n = 11, pink) were distributed within several
792 rhodopsin groups and sub-groups to determine likelihood of putative genes being of bacterial or
793 eukaryotic origins. The position of study genes is labelled by their associated /groups, with the
794 exception of genes 713097 and 1684433 being GCPR transmembrane rhodopsin associated
795 proteins, and gene 1462589 being unclear (most closely associated with the genes of
796 metagenomic origin. Bootstrap values are based off 1000 replicates and are identified if above
797 80. Abbreviations: HALO; Halorhodopsin, XANTHO; xanthorhodopsin, METAGENOME
798 RHO-LIKE; metagenomic origin rhodopsin-like putative proteins, BACTERIORHO/EUK RHO-
799 LIKE; bacteriorhodopsins and eukaryotic origin rhodopsin-like putative proteins, RHO-like;
800 sensory eukaryotic rhodopsin-like proteins. The two DE PPRs are indicated with asterisks.
801

802 **Figure 7: Bacillariophyta fasciclin transcript abundance patterns in response to ice cover.**
803 **(A)** Taxonomic distribution of DE genes categorized within COG category M (Cell wall,
804 membrane, envelope biogenesis). **(B)** COG assignments for all 354 DE genes in response to ice
805 cover, with COG category M indicated in blue. **(C)** Heatmap depicting COG category M DE
806 gene expression (VST) in response to ice cover across the 14 winter libraries. **(D)** Phylogenetic
807 tree of fasciclin distribution within diatoms. Bootstrap values above 70 are indicated with black
808 lines. The FAS1 domain was found in 141 marine and freshwater diatoms of diverse ecological
809 habitats (indicated in blue). The 18 DE diatom fasciclins in this study are indicated in purple
810 with asterisks. Bacterial fasciclins indicated in dark green), cyanobacteria (pink), chytrids (red),
811 other algae (purple), other eukaryotes (light green).
812

813 **Figure 8: Schematic representing how ice cover alters freshwater diatom colocation**
814 **strategy throughout the water column. (A)** Ice covered water column which exhibits minimal
815 convective mixing. As a result, $I_k < I_{wc}$ (where I_k = irradiance at which photosynthesis is light
816 saturated and I_{wc} = mean water column irradiance). I_{wc} is calculated based on light extinction
817 coefficient and mixing depth – which in an ice-free winter (i.e., holomictic state) is the bottom,
818 while in the presence of ice-cover, is limited to shallow convective mixing. Diatoms nucleate ice
819 and partition to the surface ice cover within the photic zone. **(B)** Ice-free water column which
820 exhibits isothermal conditions and thorough mixing. As a result, $I_k > I_{wc}$, and light-limited
821 diatoms express fasciclins to forms rafts of increased buoyancy to optimize their ability to
822 harvest light in the turbid water column. Beige colored diatoms in both diagrams represent
823 diatoms that possess PPRs, with an increased number of PPR-possessing diatoms selected for in
824 the ice-free turbid water column in panel B.



825
826
827

Figure 1

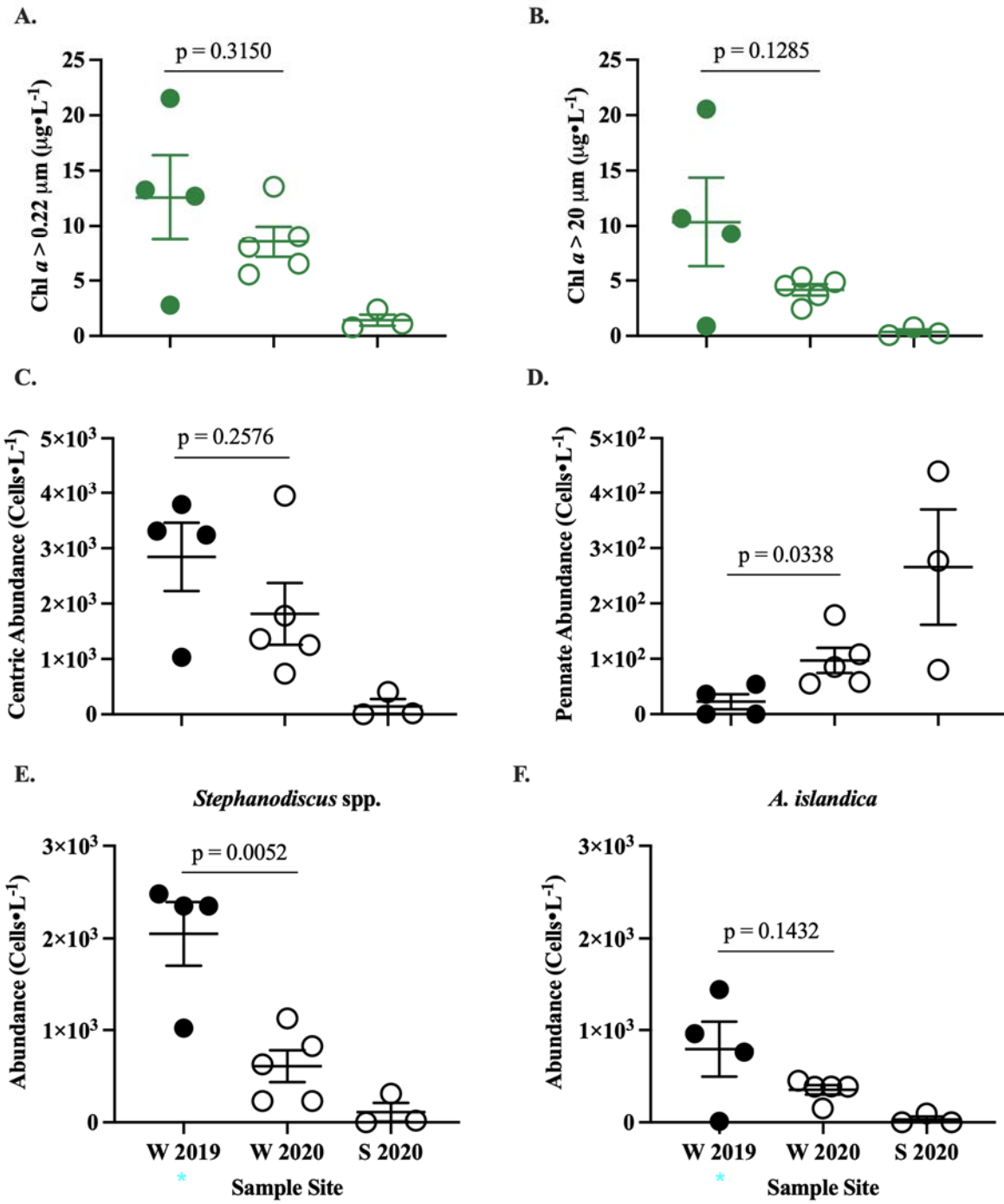


Figure 2

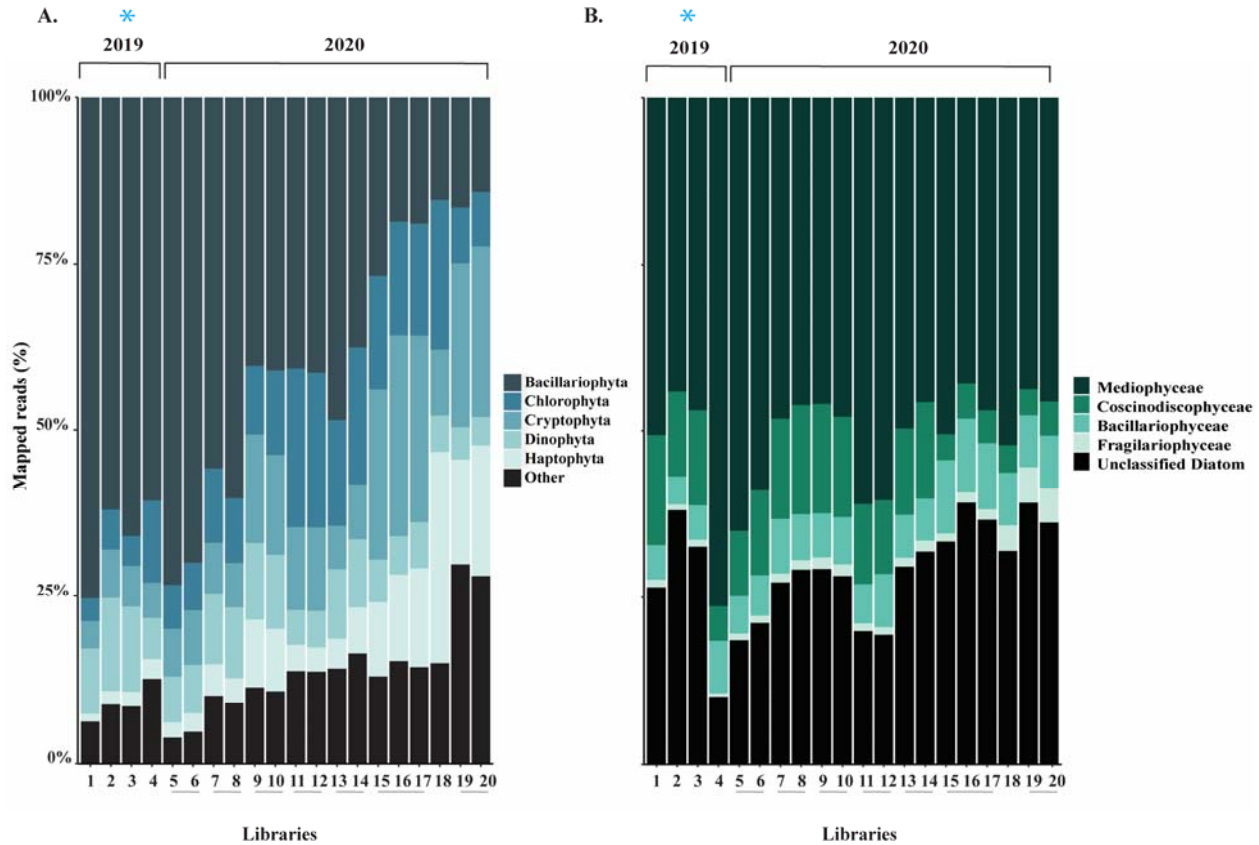


Figure 3

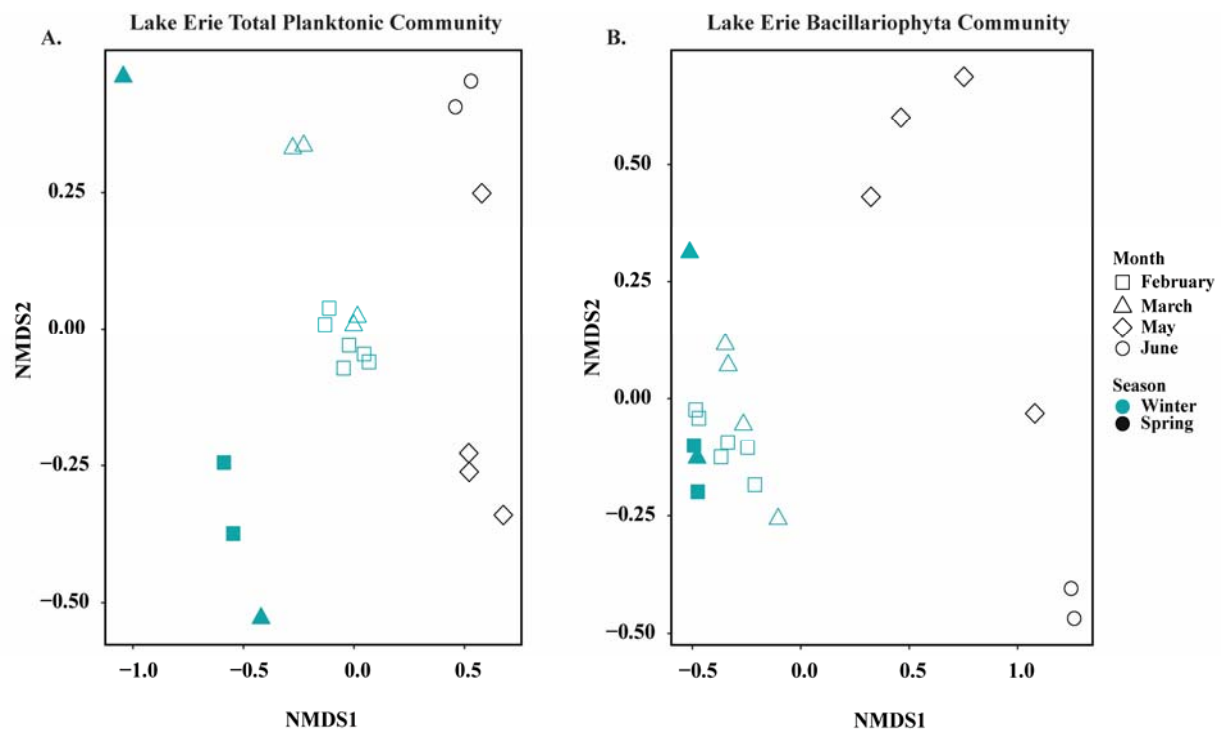


Figure 4

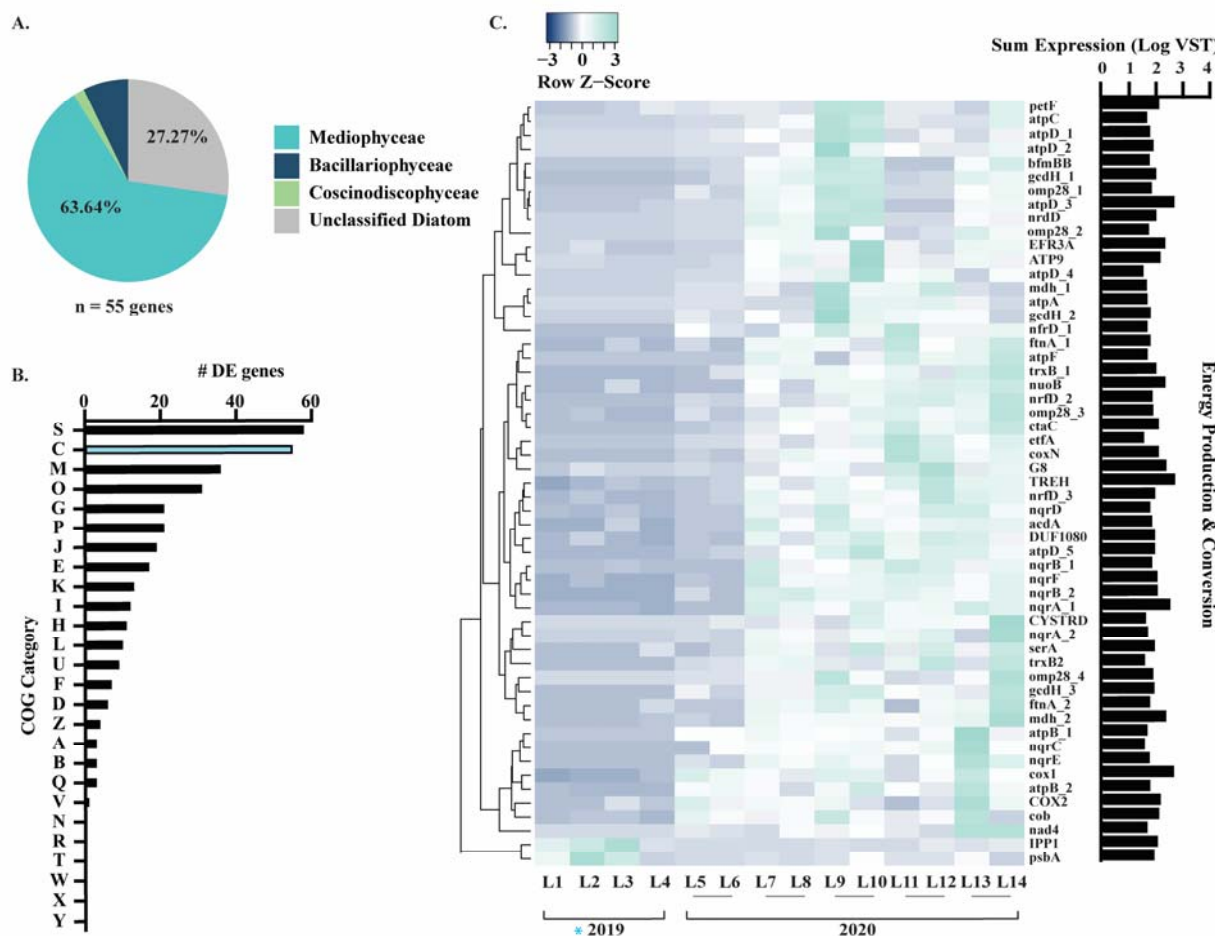


Figure 5

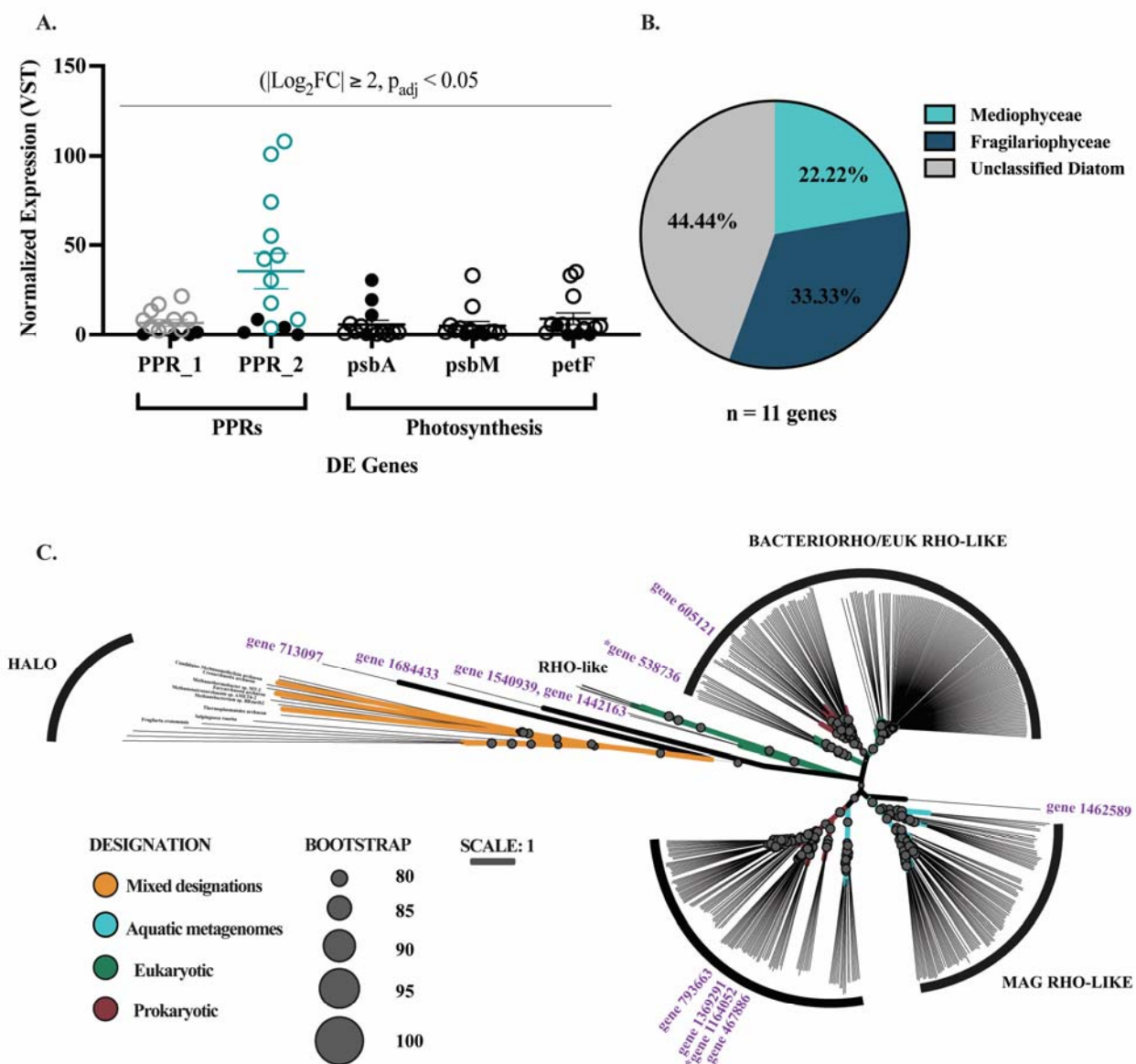


Figure 6

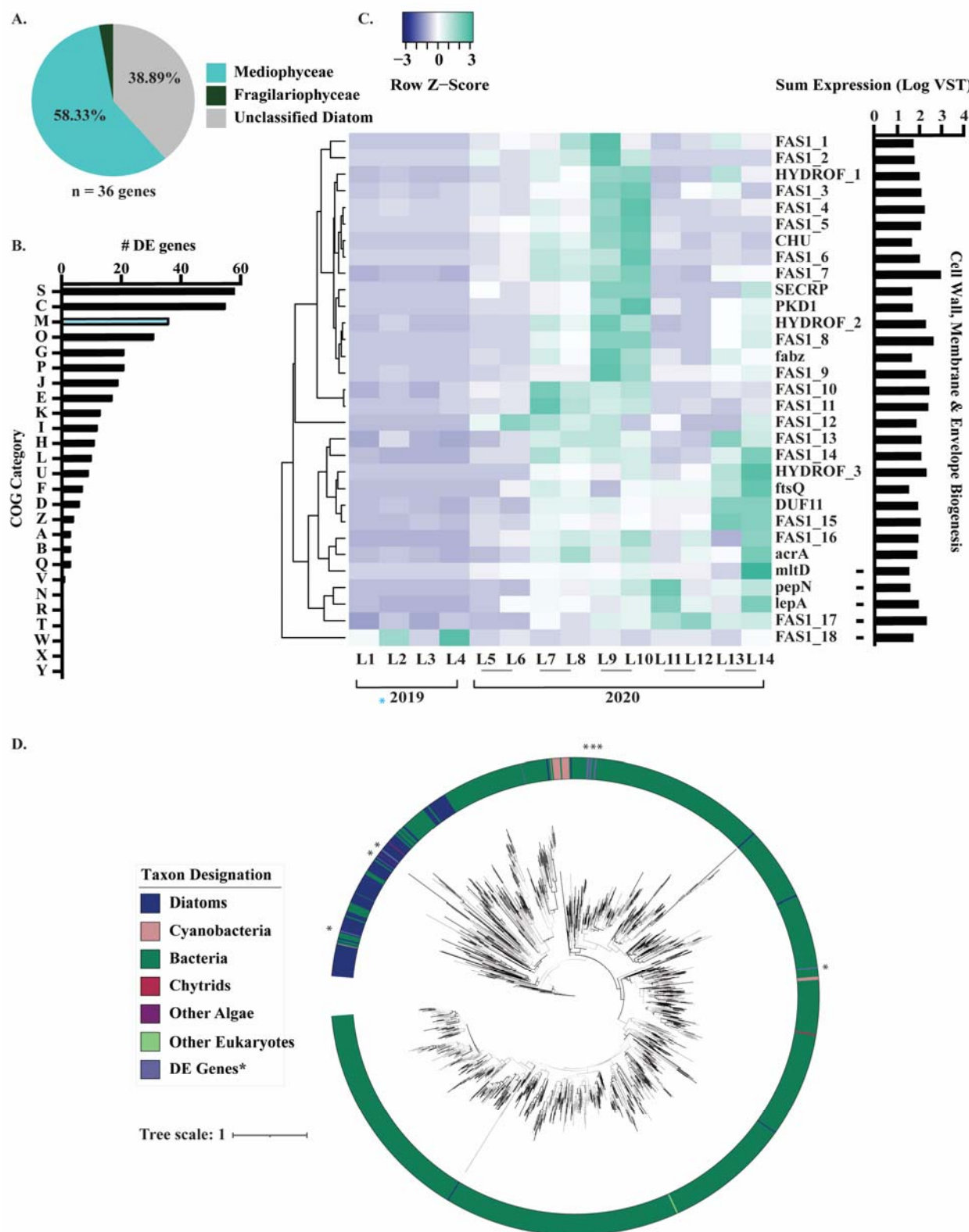


Figure 7

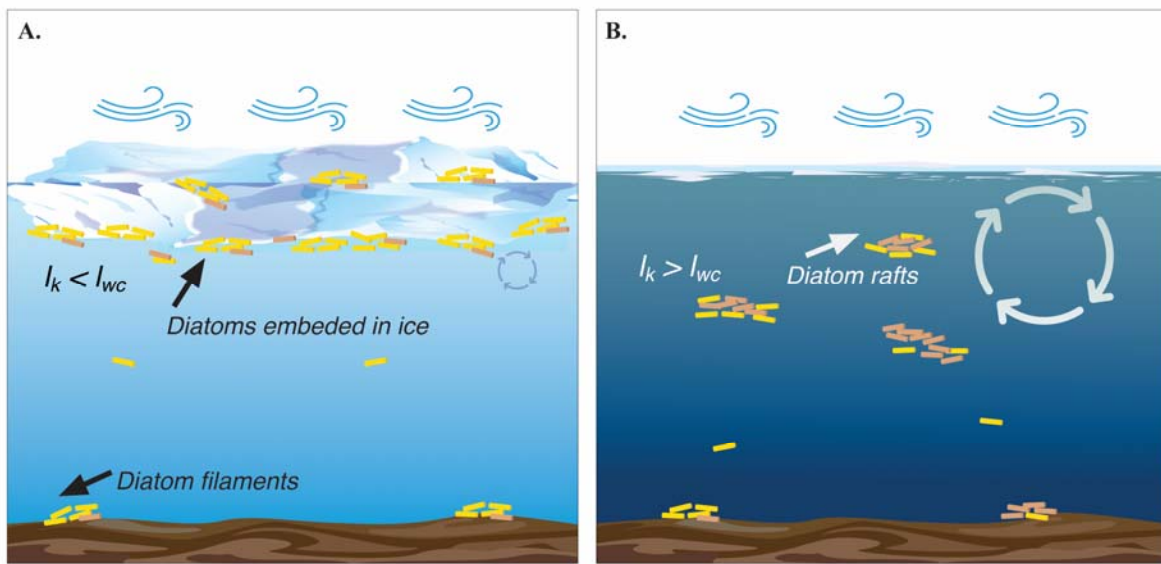


Figure 8: